Mechanisms of Signal Transduction:

Axin Inhibits Extracellular Signal-regulated Kinase Pathway by Ras Degradation via β-Catenin

Soung Hoo Jeon, Ju-Yong Yoon, Young-Nyun Park, Woo-Jeong Jeong, Sewoon Kim, Eek-Hoon Jho, Young-Joon Surh and Kang-Yell Choi

J. Biol. Chem. 2007, 282:14482-14492.
doi: 10.1074/jbc.M611129200 originally published online March 20, 2007

THE JOURNAL OF BIOLOGICAL CHEMISTRY VOL. 282, NO. 19, pp. 14482–14492, May 11, 2007

Axin Inhibits Extracellular Signal-regulated Kinase Pathway by Ras Degradation via β-Catenin*[S]

Received for publication, December 5, 2006, and in revised form, March 6, 2007 Published, JBC Papers in Press, March 20, 2007, DOI 10.1074/jbc.M611129200

Soung Hoo Jeon[‡], Ju-Yong Yoon[‡1], Young-Nyun Park[§], Woo-Jeong Jeong[‡1], Sewoon Kim[¶], Eek-Hoon Jho[¶], Young-Joon Surh[‖], and Kang-Yell Choi[‡2]

From the [‡]National Research Laboratory of Molecular Complex Control, and Department of Biotechnology, Yonsei University, Seoul 120-749, the [§]Department of Pathology, Center for Chronic Metabolic Disease, BK21 project for Medical Science, Yonsei University College of Medicine, Seoul 120-749, the [¶]Department of Life Science, University of Seoul, Seoul 130-743, and the [‖]Research Institute of Pharmaceutical Sciences, College of Pharmacy, Seoul National University, Shinlim-dong, Kwanak-ku, Seoul 151-742, Korea

Interactions between the Wnt/β-catenin and the extracellular signal-regulated kinase (ERK) pathways have been posited, but the molecular mechanisms and cooperative roles of such interaction in carcinogenesis are poorly understood. In the present study, the Raf-1, MEK, and ERK activities were concomitantly decreased in fibroblasts, which inhibit morphological transformation and proliferation by Axin induction. The inhibition of the components of the ERK pathway by Axin occurred in cells retaining wild-type β-catenin, including primary hepatocytes, but not in cells retaining non-degradable mutant β-catenin. Axin inhibits cellular proliferation and ERK pathway activation induced by either epidermal growth factor or Ras, indicating a role of Axin in the regulation of growth induced by ERK pathway activation. ERK pathway regulation by Axin occurs at least partly via reduction of the protein level of Ras. Both wild-type and mutant Ras proteins are subjected to regulation by Axin, which occurs in cells retaining wild-type but not mutant β-catenin gene. The role of β-catenin in the regulation of the Ras-ERK pathway was further confirmed by Ras reduction and subsequent inhibitions of the ERK pathway components by knock down of mutated form of β-catenin. The Ras regulation by Axin was blocked by treatment of leupeptin, an inhibitor of the lysosomal protein degradation machinery. Overall, Axin inhibits proliferation of cells at least partly by reduction of Ras protein level via β-catenin. This study provides evidences for the role of the Ras-ERK pathway in carcinogenesis caused by mutations of the Wnt/β-catenin pathway components.

The Wnt/β-catenin signaling pathway plays a crucial role in carcinogenesis as well as development (1–4). The implication of Wnt/β-catenin signaling in carcinogenesis has been attributable to aberrant regulation of this pathway as a result of mutations of the β-catenin gene, adenomatous polyposis coli (*Apc*), and/or *Axin*. Thus, mutations of these genes have been described in many types of human cancers such as hepatocellular carcinoma (5–8) and human colorectal cancer (4, 9–11). Because Apc and Axin play pivotal roles in the control and stability of β-catenin (12–15), functional alterations of these proteins can lead to accumulation of β-catenin in the nucleus and increased transcription of β-catenin/Tcf-responsive genes (16, 17). Based on these findings, mutations that constitutively stabilize and activate β-catenin are likely to be involved in malignant transformation. The ERK[3] pathway is also a major transforming pathway, and the aberrant activation of the ERK pathway by oncogenic mutation(s) such as *ras* mutation results in human cancers, including colorectal cancer and hepatocellular carcinoma (18–20). Although deregulation of both the Wnt/β-catenin and ERK pathways can lead to transformation, the interaction of the two pathways during tumorigenesis is poorly understood.

The potential tumor formation by K-*ras* mutation was significantly inhibited in cells retaining wild-type *Apc* (21). Subsequent studies have shown that β-catenin gene can cooperate with *ras* in neoplastic transformation (22, 23). Furthermore, studies utilizing colorectal cancer cell lines demonstrated that Ras-induced proliferation and transformation were reduced by overexpression of Apc (24). Although these studies imply an interaction between the Wnt/β-catenin and ERK signaling pathways in carcinogenesis, a mechanism and *in vivo* evidence for the interaction are lacking.

In this study, we investigated the relationship between the Wnt/β-catenin and the ERK pathways by measuring the effects of Axin induction using stable L929 fibroblast cells retaining doxycycline (Dox)-inducible Axin (L929-Axin). Axin, a negative regulator of Wnt/β-catenin signaling, was identified as an inhibitor of the Raf-1 → MEK → ERK cascade in fibroblasts, the

* This work was supported in part by a National Research Laboratory Grant from the Korea Science and Engineering Foundation (KOSEF) and by the Korea government (MOST) (Grants 2005-01564, 2006-02681, and R112000078010020). The costs of publication of this article were defrayed in part by the payment of page charges. This article must therefore be hereby marked "*advertisement*" in accordance with 18 U.S.C. Section 1734 solely to indicate this fact.

[S] The on-line version of this article (available at http://www.jbc.org) contains supplemental text and Figs. S1 and S2.

[1] Supported by a BK21 studentship from the ministry of education and human resources development.

[2] To whom correspondence should be addressed: Tel.: 82-2-2123-2887; Fax: 82-2-362-7265; E-mail: kychoi@yonsei.ac.kr.

[3] The abbreviations used are: ERK, extracellular signal-regulated kinase; BrdUrd, bromodeoxyuridine; Dox, doxycycline; EGF, epidermal growth factor; EGFR, EGF receptor; GFP, green fluorescent protein; EGFP, enhanced GFP; siRNA, small interference RNA; DMEM, Dulbecco's modified Eagle's medium; FBS, fetal bovine serum; FACS, fluorescence-activated cell sorting; DAPI, 4′,6-diamidino-2-phenylindole; MEK, mitogen-activated protein kinase/extracellular signal-regulated kinase kinase; TRITC, tetramethylrhodamine isothiocyanate.

finding of which was also revealed in primary hepatocytes and several cancer cells. β-Catenin was identifiable as a mediator in ERK pathway regulation by Axin, for which regulation was investigated by measurements of Axin overexpression on activation of the ERK pathway components in different types of cells that retained either a mutated or functionally active wild-type β-catenin gene. Inhibition of the ERK pathway by Axin appears to be associated with Ras regulation. The GTP-loading capacities of both mutant and wild-type Ras were reduced by Axin overexpression. The reductions of GTP loading of non-hydrolyzable mutant Ras (25) was found to be attributable to the reduction of the Ras protein level by Wnt/β-catenin signaling. The Ras regulation by Axin overexpression was abolished by treatment of leupeptin, the lysosomal inhibitor, indicating involvement of the lysosomal protein degradation machinery in the regulation of the Ras protein level.

Axin inhibits ERK pathway activation stimulated either by EGF or Ras and at least partly via reduction of Ras protein level. The Ras-ERK pathway inhibition by Axin occurs in a β-catenin-dependent manner and is related to regulation of cellular proliferation. The roles of β-catenin in the regulation of Ras and the ERK pathway components were clearly indicated by the measured effects of the knockdown of non-degradable mutant β-catenin. The role of β-catenin in Ras regulation was further indicated by the lack of effect of Axin induction in cells overexpressing β-catenin S33Y, a non-degradable β-catenin. Axin can affect Ras at the levels both of GTP loading and protein regulation. The role of EGFR in the regulation of Ras by Axin was indicated by the measured effects of *EGFR* siRNA. The functional point of Axin was further defined as occurring upstream of Raf by loss of the anti-proliferative role of Axin in cells overexpressing Raf-1-CAAX (26), an active form of Raf.

The role of Axin as the anti-transforming factor involving ERK pathway regulation was revealed by inhibition of the anchorage-independent cellular growth by EGF or oncogenic Ras in cells expressing Axin. The identification of Ras-ERK pathway regulation by Wnt/β-catenin signaling provides evidence for interaction between the Wnt/β-catenin and ERK pathways in carcinogenesis. In addition, this study also contributes to resolving the uncertainty in previous observations of a functional synergism between *ras* and β-catenin gene in carcinogenesis.

EXPERIMENTAL PROCEDURES

Plasmids—The expression vector for Axin, pCS2-MT-Axin, and inducible expression vectors for GFP (pBI-EGFP) and GFP-Axin (pBI-EGFP-Axin) were described in previous studies (14, 25). The FLAG-β-catenin-pcDNA3.0, pMT3-Ras^{L61}, pFR-Luc, and pFA2-Elk1 plasmids were described in a previous study (24). To construct a vector for *Axin* siRNA production (pAxin-siRNA), two oligomers containing the 19-nucleotide target sequences (5′-GAT CCC AGT ACA TCC TGG ATA GCA ATT CAA GAG ATT GCT ATC CAG GAT GTA CTT TTT TTG GAA A-3′ and 5′-AGC TTT TCC AAA AAA AGT ACA TCC TGG ATA GCA ATC TCT TGA ATT GCT ATC CAG GAT GTA CTG G-3′) of the murine *Axin* gene (nucleotides 827–849, GenBank^{TM} accession number AF009011) were annealed and ligated into the BglII and HindIII sites of the pSUPER vector (27). pZIP-Raf-CCAX (26) and FLAG-S33Y-β-catenin-pcDNA3.0 (28) were kindly provided by Drs. C. J. Marshall at the Institute of Cancer Research, UK, and Eric R. Fearon of the University of Michigan, respectively.

Axin-inducible Fibroblasts and Preparation of Cells—To establish GFP (L929-GFP) and GFP-Axin (L929-GFP-Axin), inducible L929 cells were co-transfected with either pBI-EGFP or pBI-EGFP-Axin with rtTA2SM2-Neo at a 1:3 molar ratio using SuperFect transfection reagent (Qiagen). Stably transfected clones were selected in a medium containing 800 μg/ml G418 (Invitrogen), and individual G418-resistant clones were isolated in cloning dishes (Sigma). L929-GFP-Axin cells were grown in Dulbecco's modified Eagle's medium (DMEM) supplemented with 10% heat-inactivated fetal bovine serum (FBS), G418 (200 μg/ml), streptomycin (100 μg/ml), and penicillin G sodium (100 μg/ml) and incubated at 37 °C in 5% CO_2. Axin was induced by 0.5 μg/ml Dox (Sigma) and/or stimulated with 20 ng/ml EGF (Cell Signaling Biotechnology). For observation of cell morphological changes, L929-Axin-GFP cells and L929-GFP cells were seeded into 6-well plates at 4×10^4 cells/well and cultured at 37 °C in 5% CO_2 for 24 h. The GFP-expressed cells were induced for 24 h by treatment with 0.5 μg/ml Dox. After induction, the cells were examined under a phase-contrast fluorescence microscope (Nikon, TE-2000U, Japan) for visualization of morphology and expression of GFP or Axin-GFP. DLD-1, HCT-116, and SW-480 colorectal cancer cells and Chang normal liver and HepG2 hepatoma cancer cells were obtained from the American Type Culture Collection and cultured as previously described (24). NIH3T3 cells containing Dox-inducible H-*ras*^{G12R} were used as described in a previous study (24). DLD-1, HCT-116, SW480, Chang, HepG2, L929, and NIH3T3 cells were seeded at 3×10^5 cells per 100-mm dish. After growth for 24 h, cells were transfected with plasmids using Lipofectamine Plus reagent according to the manufacturer's instructions (Invitrogen), and then harvested at 24 h thereafter. Cells were rinsed twice with ice-cold PBS, harvested, and then lysed using radioimmune precipitation assay buffer (Upstate, Lake Placid, NY) to determine the protein concentrations.

Primary Cells—Rat primary hepatocytes were isolated using the collagenase perfusion method (29). The portal vein was catheterized with a 22-gauge Angiocath catheter, and following perfusion of the liver with collagenase buffer, the liver was removed and shredded for isolation of hepatocytes. The hepatocytes were then washed three times with cold serum-free DMEM. Hepatocytes (1.5×10^6) were seeded onto 60-mm dishes coated with collagen IV (BD Biosciences) and cultured in DMEM with 10% FBS, streptomycin (100 μg/ml), and penicillin G sodium (100 μg/ml) then incubated at 37 °C in 5% CO_2. To examine the effects of Axin and/or EGF, cells were transiently transfected with pCS2-MT-Axin and/or were treated with 20 ng/ml EGF. The cells were harvested at 24 h after transfection and subjected to Western blot analysis.

β-Catenin and EGFR siRNAs and Treatment—β-Catenin gene (GenBank^{TM} accession number NM_001904) and *EGFR* (NM_207655) mRNA target sequences were designed using an siRNA template design tool (Ambion, Austin, TX), and siRNA was prepared with a Silencer^{TM} siRNA construction kit

(Ambion), as described previously (24). 29-mer oligonucleotides containing the T7 promoter sequence (5′-CCTGTCTC-3′) were designed (mouse *EGFR*, 5′-AATGGACTTACAGAG-CCATCC-3′ (531–551) and 5′-AAAGAAGACGCCTTCTTG-CAG-3′ (3181–3201); human β-catenin gene, 5′-AAGGAGC-TAAAATGGCAGTGC-3′ (800–821) and 5′-AATGGCTTG-GAATGAGACTGC-3′ (2061–2082)). The siRNAs were transfected into HCT-116 or L929-Axin cells with Lipofectamine Plus reagent, using an 8.4 μg per 100-cm culture dish. The transfected cells were grown for 36 h at 37 °C in a 5% CO_2 incubator and harvested for Western blot analysis.

Western Blot Analysis—Western blot analysis was performed as previously described (7). Anti-Axin (Upstate), -β-catenin, -active β-catenin (αABC) (Upstate), -p-Akt (Santa Cruz Biotechnology, Santa Cruz, CA), -Pan-Ras cloneRAS10 (Upstate), -p-Raf-1 serine 338 (Upstate), -p-MEK, -p-p38 (Cell Signaling Biotechnology), -p-ERK (Santa Cruz Biotechnology), -ERKs (Santa Cruz Biotechnology), -cyclin D1 (Santa Cruz Biotechnology), and -α-tubulin (Oncogene) primary antibodies were used followed by incubation with horseradish peroxidase-conjugated secondary antibody (Santa Cruz Biotechnology). Protein bands were visualized by enhanced chemiluminescence (Amersham Biosciences).

Foci Formation Assay—To evaluate anchorage-independent growth, 1.2×10^3 L929-Axin-GFP cells were suspended in 1 ml of 0.3% molten top agarose (Invitrogen) with or without 0.5 μg/ml Dox and overlaid onto 1 ml of 0.5% solid bottom agarose in 12-well plates. After solidification, the top layer of agarose was covered with 1 ml of culture medium with and without 0.5 μg/ml Dox and, where required, 20 ng/ml EGF was added. The colonies were maintained at 37 °C and periodically replenished with fresh medium containing Dox and/or EGF. Fourteen days after plating, colonies were examined under a phase-contrast fluorescence microscope for visualization of colonies expressing GFP. Whole well images were captured using a Nikon digital camera and viewed using Adobe Photoshop 7.0 software. The average size of globes was calculated by averaging data (data are expressed as mean, μm^3) from at least 150 colonies. Differences between groups were analyzed using the two-sample *t* test and were considered significant when the *p* value was <0.05. To measure the effect of Axin in anchorage-independent Ras-induced growth, NIH3T3-H-Ras^{G12R} cells (24) were transfected with pCS20MT-Axin for 24 h, 1.5×10^3 cells were then re-seeded into a 12-well soft agar plate, as described above, and H-Ras^{G12R} was induced with Dox, also as described above.

Cell Cycle and Quantitative Proliferation Analyses—The cell cycle was analyzed by fluorescence-activated cell sorting (FACS) as previously described (24). L929-GFP-Axin cells were grown to 60% confluence in 6-well plates and were arrested with double thymidine blocking for 12 h. Cells were then either untreated or treated with 0.5 μg/ml Dox and/or 20 ng/ml EGF at 12 h before FACS analysis. Cells were harvested, rinsed twice with PBS, fixed in 70% ice-cold ethanol, and then washed in PBS containing 1% FBS. Subsequently, DNA was stained with propidium iodide (BD Biosciences) for 30 min at 37 °C. The cell cycle profile was determined using a FACSCalibur (BD Biosciences). Data were analyzed using the ModFit LT 2.0 program (Verity Software House, Inc., Topsham, ME) and the WinMDI 2.8 program created by Joseph Trotter of Scripps Research Institute. Error bars indicate the standard deviations of three independent analyses experiments.

For quantitative analyses of proliferation, L929-GFP-Axin cells were transfected with pZIP-Raf-CCAX (26) for 24 h followed by subsequent induction of Axin with 0.5 μg/ml Dox for 24 h at 37 °C in 5% CO_2. BrdUrd addition and measurements of the relative intensities of BrdUrd were performed as described previously (24).

Cell Growth Measurement—Cell growth was determined by the number of viable cells. The cells were seeded into 6-well plates at 2×10^4 cells/well, and the medium was replaced every day with fresh DMEM containing 10% FBS with or without 0.5 μg/ml Dox. Where required, 20 ng/ml EGF was added. For enumeration of viable cells, cells were trypsinized and washed once with PBS, and then the total numbers of viable cells were counted using a hemocytometer.

BrdUrd Incorporation—For BrdUrd incorporation, L929 or NIH3T3-Ras cells were seeded onto 22 × 22-mm coverslips in 6-well plates at 2×10^4 cells per well. Cells were transiently transfected with pCS2-MT-Axin, pCS2-MT, FLAG-β-catein-pcDNA3.0, or pcDNA3.0 and treated with 0.5 μg/ml Dox for H-Ras induction. Where required, BrdUrd (Roche Applied Science) was added at a final concentration of 20 μM at 36 h after transfection, and the cells were further incubated for 8 h at 37 °C. Cells were washed twice with PBS and then fixed in a methanol/formaldehyde (99:1, v/v) mixture at −20 °C for 20 min. Cells were permeabilized with 0.2% Triton X-100 at 4 °C for 30 min and then gently washed three times with PBS. Cells were incubated with mouse anti-BrdUrd monoclonal antibody (DAKO, Carpinteria, CA) at a 1:100 dilution for 2 h at room temperature, incubated with goat anti-mouse-Cy™2-conjugated secondary antibody at a 1:1000 dilution for 1 h at room temperature, and then washed five times with PBS. For nuclear staining, 4′,6′-diamidine-2′-phenylindole dihydrochloride (DAPI, Roche Applied Science) was used at a final concentration of 1 μg/ml in PBS for 10 min followed by extensive washing with PBS. Coverslips were mounted, and then cells were viewed using a Radiance 2000/MP multiphoton imaging system (Bio-Rad). Each analysis was performed at least three times.

Measurement of Ras Activation—The capacity of Ras-GTP to bind the Ras binding domain of Raf-1 was used to determine the level of GTP-bound Ras, as described previously (24).

Reporter Analysis—For reporter gene assays, L929-GFP-Axin cells were seeded into 6-well dishes at 2×10^4 cells per well. Transfection efficiencies were determined by transfecting cells with 50 ng of the β-galactosidase reporter plasmid, pCMV β-galactosidase (Clontech). L929-GFP-Axin cells were co-transfected with 0.5 μg of pElk-1, 0.5 μg of pFR-Luc, and 25 ng of pFA2-Elk-1. At 48 h after transfection, cells were harvested and luciferase assay were performed in triplicate from independent cell cultures as described previously (24).

Immunocytochemical Staining—For immunocytochemical staining, L929-Axin-GFP cells were seeded at 2×10^4 cells/well in 6-well plates on 22 × 22-mm coverslips and cultured for 24 h at 37 °C in 5% CO_2. The cells were treated with 0.5 μg/ml Dox. Induced L929-Axin-GFP cells were fixed for 15 min at room temperature with 3.7% paraformaldehyde in PBS at pH 7.4, per-

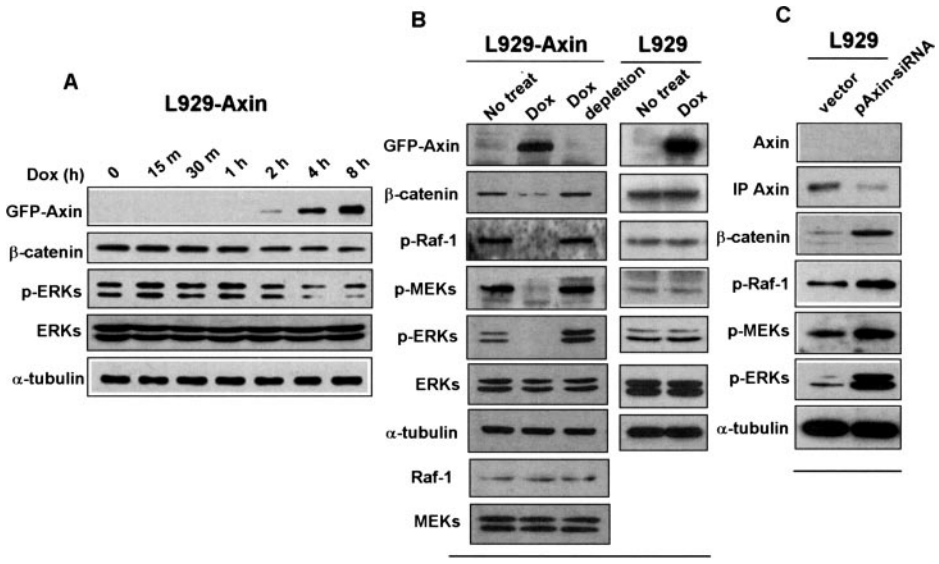

FIGURE 1. **Effects of Axin overexpression on the activation of ERK pathway of L929 cells.** *A*, L929-GFP-Axin cells were grown in DMEM supplemented with 10% heat-inactivated FBS, G418 (200 μg/ml), streptomycin (100 μg/ml), and penicillin G sodium (100 μg/ml) in 5% CO_2 at 37 °C. Axin was induced by 0.5 μg/ml Dox treatment for the indicated times. Cell extracts were resolved on 10% SDS-PAGE, and GFP-Axin, β-catenin, p-ERKs, ERKs, and α-tubulin proteins were detected by Western blot analysis. *B*, L929-GFP-Axin (*left panel*) and L929-GFP (*right panel*) cells were either untreated or treated with 0.5 μg/ml Dox for 48 h. Where required, cells grown for 24 h in the presence of 0.5 μg/ml Dox were further grown for an additional 24 h in an identical fresh medium depleted of Dox (*right lane*). GFP-Axin, β-catenin, p-Raf-1, p-MEK, p-ERK, ERKs, Raf-1, MEK, and α-tubulin were detected by Western blot analysis. *C*, L929 cells were grown to 3×10^5 confluence and transiently transfected with either an empty vector or the *Axin* siRNA vector, as described under "Experimental Procedures." Axin, β-catenin, p-Raf-1, p-MEK, p-ERK, and α-tubulin were monitored by Western blot analyses at 48-h post-transfection. Axin was detected by immunoprecipitation (*IP*) of 400 μg of whole cell lysate with anti-Axin antibody followed by Western blot analysis.

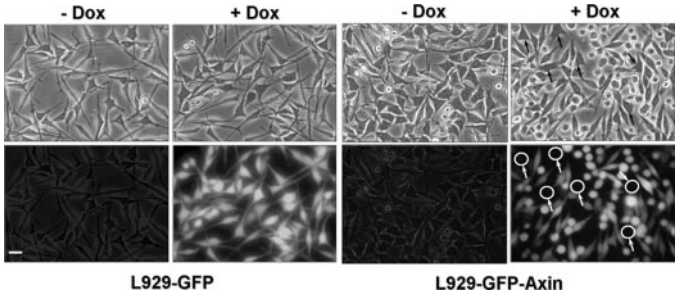

FIGURE 2. **Effects of Axin overexpression on the morphology of L929 cells.** L929-GFP-Axin and L929-GFP cells were grown in 6-well plates, as described under "Experimental Procedures." Cells were untreated or treated with 0.5 μg/ml Dox for 24 h. The cells were viewed at ×200 magnification under a fluorescence microscope and photographed. The *arrows* indicate cells maintaining polygonal morphology due to no GFP-Axin induction. *Bar*, 50 μm.

meabilized for 30 min on ice with 0.2% Triton X-100 in PBS, and blocked with 1% bovine serum albumin overnight at 4 °C. The antibody and DAPI reactions used the same fluorescence staining method. Following several washing with PBS, the slides were mounted in a mounting medium. Cells were imaged using a Radiance 2100 laser scanning confocal microscope and operated by Lasersharp 2000 software (Bio-Rad). A minimum of three 0.5-μm Z slices were acquired for each cell.

RESULTS

Axin Inhibits the ERK Pathway and Alters the Morphology of L929 Fibroblasts—The role of Wnt/β-catenin signaling in ERK pathway regulation was investigated by examining the effects of Axin on the activities of the ERK pathway components. For this purpose, we generated L929 cells expressing Axin by a Dox-inducible system (L929-GFP-Axin). Upon treatment with Dox, expression of GFP-Axin was evident in L929-GFP-Axin cells after 2 h and was sustained up to 8 h post-induction (Fig. 1*A*). There was a concomitant reduction in β-catenin protein levels and ERK phosphorylation upon GFP-Axin induction (Fig. 1*A*). The phosphorylation of upstream regulators of ERK, such as Raf-1 and MEK, were also reduced by GFP-Axin induction (Fig. 1*B*). Phosphorylation of the ERK pathway components and the level of β-catenin were restored in cells grown in fresh Dox-depleted medium (Fig. 1*B*, *left panel*), indicating that co-regulation of β-catenin and ERK signaling is a reversible process. The β-catenin and ERK pathway components were not affected by induction of GFP in L929-GFP cells (Fig. 1*B*, *right panel*). The levels of phosphorylated Raf-1, MEK, and ERK were elevated in cells expressing increased levels of β-catenin due to *Axin* siRNA (Fig. 1*C*), confirming the negative role of Axin in ERK activation. The level of endogenous Axin was low due to rapid protein turnover (30), but the low level was detectable when the protein extracts were enriched by immunoprecipitation (Fig. 1*C*).

Murine L929 cells display fibroblast morphology characterized as the polygonal/cuboidal phenotype with projection of long, sharp spikes at the cellular periphery. GFP expression alone did not significantly change the cellular morphology (Fig. 2, *left two panels*). However, expression of GFP-Axin resulted in an altered cellular morphology characterized by a spindle (bipolar) or globular shape (Fig. 2, *right two panels*). L929-GFP-Axin cells that failed to express GFP-Axin upon Dox treatment (marked by *arrows*) retained the typical polygonal morphology of L929 cells (Fig. 2).

Axin Inhibits the G_1 to S Phase Cell Cycle Progression and Growth of L929 Fibroblast Cells Stimulated by EGF—To determine whether Axin affects proliferation via the ERK pathway, we measured the effect of Axin expression on G_1 to S phase cell cycle progression stimulated by EGF. EGF treatment increased the proportion of cells in the S phase from 43% to 58% (Fig. 3*A*). The increase was abolished after introduction of GFP-Axin (Fig. 3*A*, representative data are shown in the *lower panel*). EGF with 96-h post-treatment increased the cell numbers 3-fold compared with the untreated cells (Fig. 3*B*, *upper panel*). However, the Dox-induced growth stimulation was reduced 70% in cells expressing GFP-Axin (Fig. 3*B*, *upper panel*). Treatment of L929-GFP cells with Dox alone did not affect the cell number

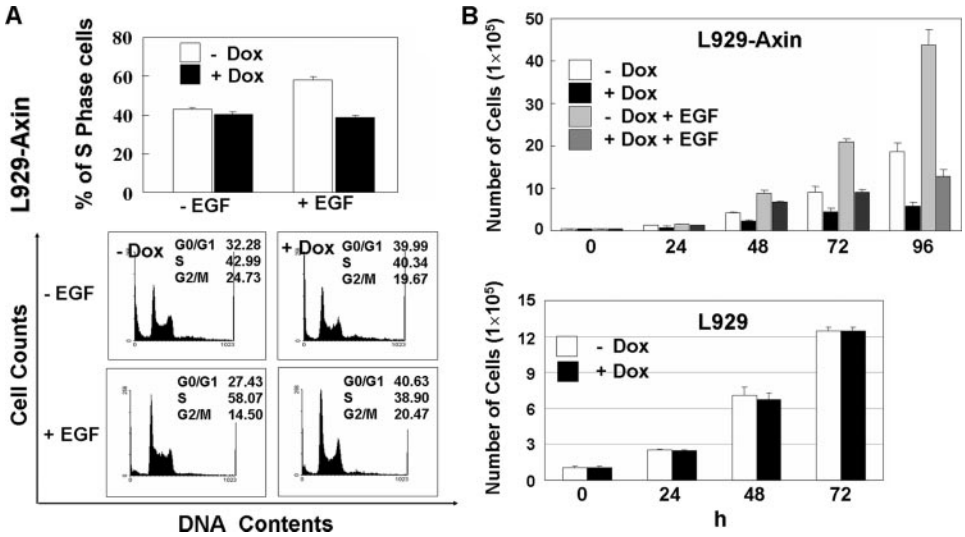

FIGURE 3. **Effects of Axin on EGF-induced G_1 to S phase cell cycle progression and growth of L929 cells.** *A*, L929-GFP-Axin cells were grown in DMEM and synchronized with double thymidine blocking for 12 h. Where required, the cells were treated with 0.5 μg/ml Dox and/or 20 ng/ml EGF 12 h before fixing for FACS analysis. *Upper panel*: relative percentage of cells in the S phase. *Error bars* indicate the standard deviations of three independent analyses. *Lower panel*: representative data for the cell cycle profile. *B*, L929-GFP-Axin (*upper panel*) and L929-GFP (*lower panel*) cells were grown in DMEM containing 10% FBS at a 2×10^4 cells per well in 6-well plate. Cells were treated with 0.5 μg/ml Dox and/or 20 ng/ml EGF every 12 h, and cell numbers were counted at different times (0, 24, 48, 72, and 96 h). *Error bars* indicate the standard deviations of three independent analyses.

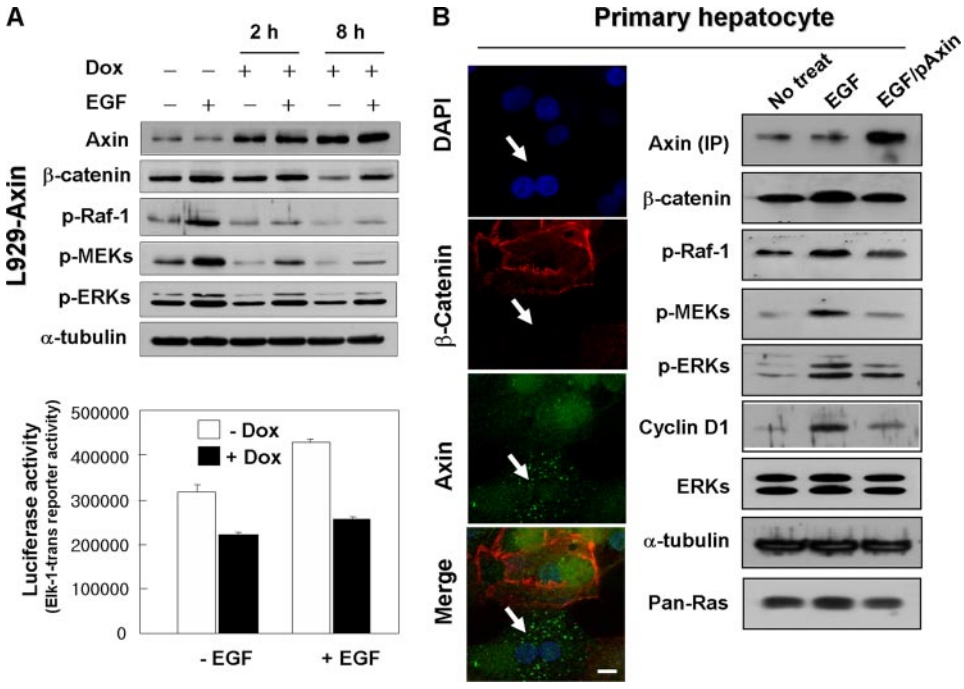

FIGURE 4. **Effects of Axin on the EGF-induced activation of the ERK pathway.** *A*, effects of Axin on the EGF-induced ERK activation and transcriptional activity. *Upper panel*, L929-GFP-Axin cells were grown in DMEM with or without 0.5 μg/ml Dox for either 2 or 8 h. EGF at 20 ng/ml was added to cells 2 h before harvesting, where required. Western blot analysis was performed on cell lysates for detection of Axin, β-catenin, p-Raf-1, p-MEK, p-ERK, and α-tubulin. *Lower panel*, L929-GFP-Axin cells were transfected with 0.5 μg of Elk-1 together with 0.5 μg of pFR-Luc and 25 ng of pFA2-Elk-1. EGF at 20 ng/ml was added to cells 2 h before harvesting. Cells were harvested 48 h post-transfection, and relative reporter activities were measured by a luciferase assay. Each data point represents the average of three independent analyses. *Error bars* indicate the standard deviations of three independent analyses. In *B*: *Left*, primary hepatocytes were transfected with pCS2-MT-Axin for 48 h. The cells were then treated with anti-β-catenin and anti-Axin antibodies. β-Catenin proteins were detected as a *red color* using anti-mouse-Rhodamine Red™, Axin proteins were detected as a *green color* using anti-mouse-fluorescein isothiocyanate. The cell nuclei were stained with DAPI. Samples were mounted for photography on a confocal microscope as described under "Experimental Procedures." *Bar*, 10 μm. In *B*: *Right*, primary hepatocytes were transfected with pCS2-MT or pCS2-MT-Axin for 48 h. Cells were then untreated and treated with 20 ng/ml EGF 2 h before harvesting. Western blot analysis was performed to detect β-catenin, p-Raf-1, p-MEK, p-ERK, ERKs, Pan-Ras, Cyclin D1, and α-tubulin. Axin was detected by immunoprecipitation (*IP*) of 400 μg of whole cell lysate followed by detection by Western blot analysis.

(Fig. 3*B*, *lower panel*), indicating that Dox alone does not inhibit L929 cell growth.

Axin Inhibits EGF-induced Activation of the ERK Pathway in L929 Fibroblast Cells and in Primary Hepatocytes—To confirm the role of the ERK pathway in anti-proliferation by Axin, we monitored the effect of Axin induction on activations of ERK pathway components. The phosphorylation levels of Raf-1, MEK, and ERK kinases that were concomitantly increased upon EGF treatment were reduced by GFP-Axin induction followed by a 2-h Dox treatment (Fig. 4*A*, *upper panel*). The effects of Axin on the EGF-induced activation of ERK signaling were further potentiated by the sustained Dox treatment up to 8 h, despite the presence of EGF. Elk-1-mediated reporter gene activation by EGF was also reduced upon Axin induction (Fig. 4*A*, *lower panel*). Therefore, Axin inhibits the ERK pathway activation that is caused by EGF. We also observed a minor increase in β-catenin protein levels at 2 h after EGF treatment, which was reduced by GFP-Axin induction (Fig. 4*A*, *upper panel*).

To examine the effect of *Axin* on ERK pathway regulation under a more physiologically relevant condition, we used primary hepatocytes in measuring the Axin effect on ERK pathway regulation. The endogenous β-catenin was mostly localized at the cell-cell boundaries and was mostly eliminated in cells overexpressing Axin by transient transfection (Fig. 4*B*, *left panel*; cells producing Axin in particulate forms are marked by a *white arrow*), indicating the functionality of transfected *Axin* in primary hepatocytes. Phosphorylation of Raf-1, MEK, and ERK kinases and β-catenin protein levels were concomitantly increased after EGF treatment but were reduced in cells with overexpressed Axin (Fig. 4*B*, *right panel*). Cyclin D1 expression, which is subject to regulation by both the Wnt/β-catenin and ERK signaling pathways (31) was increased by EGF treatment, and again was significantly reduced by Axin overexpres-

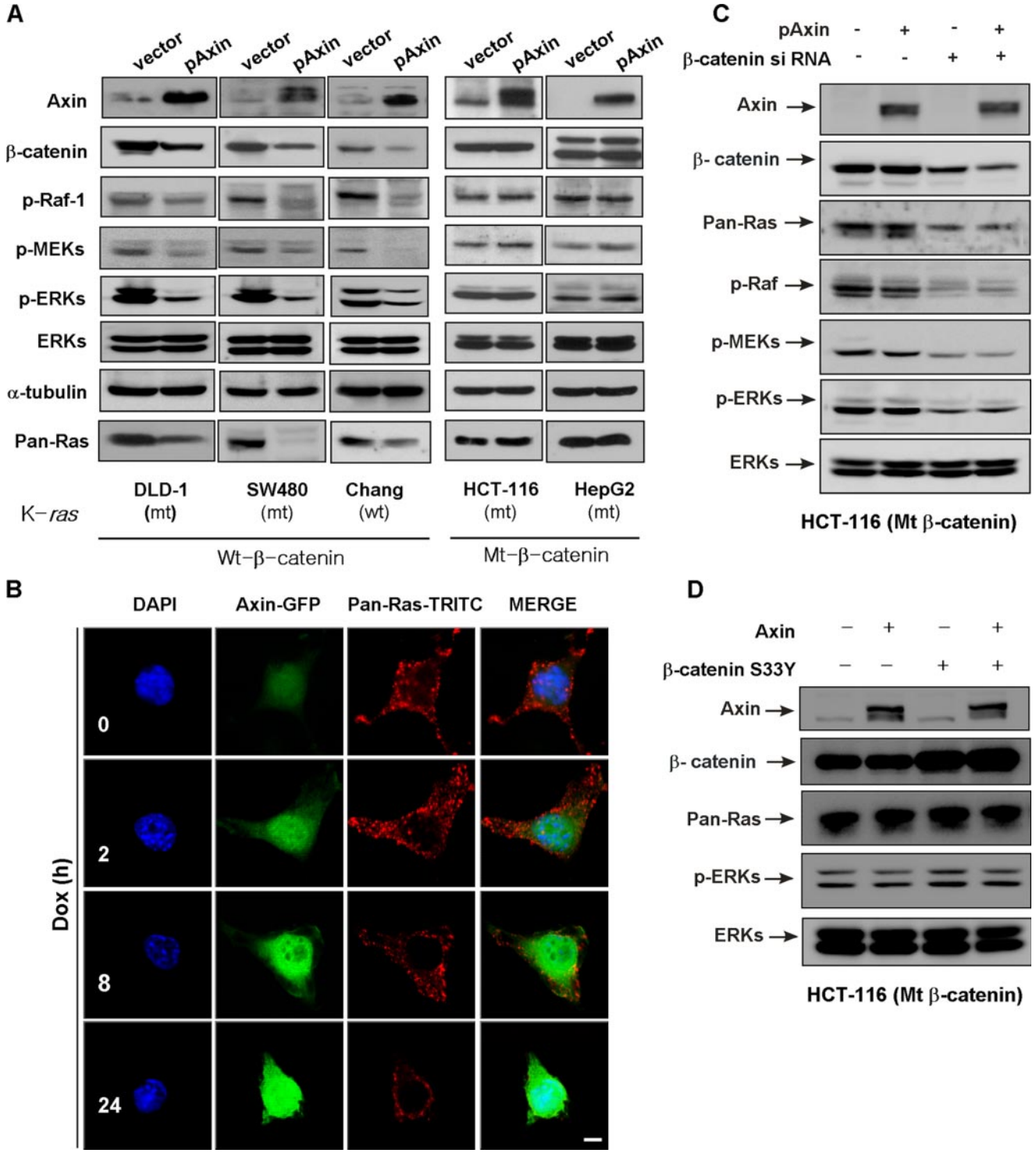

FIGURE 5. **Effect of Axin overexpression in cells either retaining wild-type or mutant β-catenin gene.** *A*, effect of Axin on Ras-ERK pathway activation in cells that retained a different genetic status of β-catenin gene. Cells that retained wild-type β-catenin gene (DLD-1 or SW-480 colorectal cancer cells, and Chang liver cells) or that retained mutated β-catenin gene (HCT-116 or HepG2 cells) were transfected with the pCS2-MT vector or pCS2-MT-Axin. The levels of Axin, β-catenin, p-Raf-1, p-MEK, p-ERK, ERK, α-tubulin, and Pan-Ras were detected by Western blot analyses at 48 h after transfection. *B*, immunocytochemical analysis of Ras regulation by Axin. L929-GFP-Axin cells were grown in DMEM and infected with retroviral H-*ras*, and cells were induced 0.5 μg/ml Dox for 0, 2, 8, and 24 h. Cells were incubated with anti-Pan-Ras antibody followed by labeling with anti-mouse rhodamine for Ras detection. GFP-Axin was visualized as GFP by confocal microscopic analysis. Cell nuclei were stained with DAPI. *Bar*, 10 μm. *C*, effect of β-catenin gene siRNA on Ras-ERK pathway regulation in HCT-116 cells that retained mutated β-catenin gene. HCT116 cells were transfected with the pCS2-MT vector or pCS2-MT-Axin together with (or without) control or β-catenin gene siRNA. The levels of Axin, β-catenin, Pan-Ras, p-Raf-1, p-MEK, p-ERK, and total ERK were detected by Western blot analyses 48 h after transfection. *D*, effect of β-catenin gene-S33Y, a non-degradable form of β-catenin, on Ras-ERK pathway regulation in HCT-116 cells. HCT116 cells were transfected with the pCS2-MT vector or pCS2-MT-Axin together with (or without) the pcDNA3.0 vector or FLAG-S33Y-β-catenin gene-pcDNA3.0. The levels of Axin, β-catenin, Pan-Ras, p-ERK, and total ERK were detected by Western blot analyses 24 h after transfection.

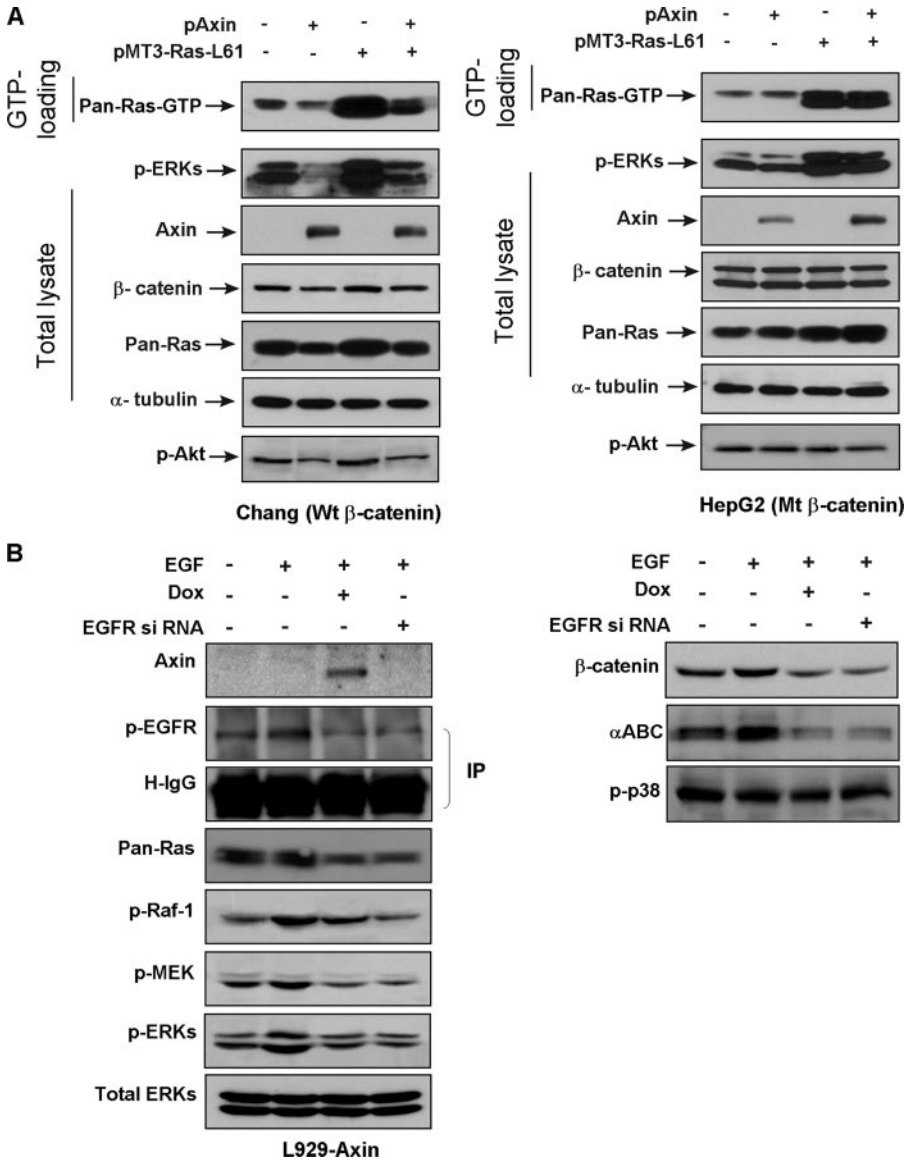

FIGURE 6. **Effect of Axin overexpression on Ras-ERK pathway activation by H-Ras^{L61} and effect of EGFR knockdown on β-catenin and Ras-ERK pathway regulation by Axin.** *A*, effect of Axin on Ras-ERK pathway activation in cells that retained wild-type or overexpressed non-degradable mutant Ras. Chang liver (*left*) and HepG2 (*right*) cells were grown and transiently transfected with a combination of pCMV, pAxin, and pMT3-H-Ras^{L61}. The GTP loading analysis was performed to detect GTP-bound Ras (Ras-GTP), as described under "Experimental Procedures." The levels of Pan-Ras-GTP, p-ERK, Axin, β-catenin, Pan-Ras, p-Akt, and α-tubulin were detected by Western blot analyses. *B*, effect of *EGFR* siRNA on β-catenin and Ras-ERK pathway regulation by Axin. L929-GFP-Axin cells were transfected with control or *EGFR* siRNA. The cells were treated with 0.5 μg/ml Dox and/or 20 ng/ml EGF for 12 h and 10 min, respectively, before harvesting them in the required case. The levels of Axin, p-EGFR, Pan-Ras, p-Raf-1, p-MEK, p-ERK, ERK, β-catenin, αABC (anti-active β-catenin) (37), or p-p38 were detected by Western blot analyses. The p-EGFR blot was obtained by Western blot analyses with the samples immunoprecipitated by 2 μg of anti-EGFR antibody against 600 μg of total lysates with Protein A beads.

sion. Again, endogenous Axin was only detected only after enrichment by immunoprecipitation.

The ERK Pathway Was Regulated by Axin in a β-Catenin-dependent Manner—Axin functions through ubiquitin-dependent degradation of β-catenin (12, 32). To identify the role of β-catenin in the Axin-induced inhibition of the ERK pathway, we measured the effects of Axin on ERK pathway components in several different cell types either expressing wild-type or non-degradable mutant β-catenin. Phosphorylations of Raf-1, MEK, and ERK kinases were reduced by transient transfection of intact *Axin* into DLD-1 and SW-480 colorectal cancer cells and Chang liver cells that retained wild-type β-catenin gene (Fig. 5*A*). However, the Axin-induced ERK pathway regulation was abolished in HCT-116 colorectal cancer and HepG2 hepatocarcinoma cells expressing a mutated β-catenin gene (5, 33), showing that β-catenin is required for ERK pathway inhibition by Axin. The β-catenin in HepG2 that lacks a potential phosphorylation site for glycogen synthase kinase-3β (34) is detectable as two bands by using anti-β-catenin antibody when visualized by Western blot analyses (Fig. 5*A*). We also investigated the effect of Axin induction on Ras protein by immunocytochemical analysis. Ras protein overexpressed by the retroviral transfection system was mostly localized in the cytoplasm and membrane area of L929-GFP-Axin cells (Fig. 5*B*). The level of Ras protein overexpressed was decreased stepwise by increasing the Axin induction time up to 24 h. The Ras protein remained only in the perinuclear area of cells at 24 h after induction with Dox (Fig. 5*B*). To provide clear evidence for the regulation of the Ras protein level by Axin, we measured the effects of β-catenin knockdown in HCT-116 cells retaining mutated β-catenin (Fig. 5*C*). The levels of Ras and active ERK pathway components (p-Raf-1, p-MEK, and p-ERKs) were simultaneously decreased by siRNA-mediated reduction of β-catenin. Here, Axin did not affect the level of Ras or the activities of the ERK pathway components (Fig. 5*C*). Finally, Ras regulation was not observed in HCT-116 cells overexpressing β-catenin-S33Y, a non-degradable form of β-catenin (Fig. 5*D*). Therefore, regulation of the β-catenin protein level is an essential factor in the regulation of Ras and ERK pathway components. Although β-catenin is involved in Ras regulation, neither the Ras protein level nor the ERK activities were increased by β-catenin-S33Y.

Suppression of the ERK Pathway by Axin Occurs at Least Partly via the Reduction of the Ras Protein Level—We measured the effect of Axin overexpression on Ras activation to further characterize the involvement of Ras, the upstream component of the ERK pathway, in ERK pathway regulation by Axin. The

Ras activity monitored by GTP loading of Ras (Ras-GTP) was significantly increased by H-Ras^{L61} overexpression, and was inhibited by Axin co-expression in Chang cells but not in HepG2 cells, which retain wild-type and mutant β-catenin gene, respectively (Fig. 6*A*, compare *left* and *right panels*). The reduction of GTP-Ras^{L61}, the GTP-bound form of non-hydrolysable Ras^{L61} (35), by Axin, was surprising and indicated the possibility of the regulation of Ras according to protein level. The level of Pan-Ras, which was increased by H-Ras^{L61} overexpression, was reduced by Axin co-expression, and that also occurred in Chang cells but not in HepG2 cells (Fig. 6*A*, compare *left* and *right panels*). The -fold regulations of Ras protein levels by Axin, however, were much lower than that of Ras-GTP by Axin. The increases in the levels of GTP-Ras and Ras by H-Ras^{L61} overexpression were similarly reduced by Axin co-overexpression in NIH3T3 cells that also retained wild-type β-catenin (data not shown, supplemental Fig. S1). The level of endogenous Ras was also reduced by Axin overexpression in Chang, DLD-1, and SW-480 cells (Fig. 5*A*) as well as in primary hepatocytes (Fig. 4*B*). By contrast, endogenous Ras levels were not reduced in HepG2 and HCT-116 cells that retained mutated β-catenin gene (Fig. 5*A*). Akt is one of the Ras effectors (36); accordingly, the p-Akt level was increased by Ras^{L61} and blocked by Axin induction (Fig. 6*A*). The patterns of p-Akt regulation by Ras^{L61} and Axin are similar to those by β-catenin and Ras. Akt regulation by Axin or Ras, however, was not observed in cells retaining mutant β-catenin gene (Fig. 6*A*, *right panel*). The level of p-Akt was not increased by Ras^{L61} in HepG2 cells by an unknown mechanism, but that did not affect the quality of the results (Fig. 6*A*, *right panel*).

EGFR Is Involved in the Regulation of Ras and the ERK Pathway Components by Axin—To identify the involvement of EGFR in Ras regulation by Axin, we measured the effects of *EGFR* siRNA (Fig. 6*B*). The p-EGFR levels, which were detected only after enrichment by immunoprecipitation of EGFR, were increased by 10-min stimulation with EGF in L929 cells, indicating the functionality of EGF. It was noticeable that the Ras protein level did not change, although the p-Raf-1, p-MEK, and p-ERKs levels were increased by 10-min EGF treatment. Interestingly, we noticed an increase of non-phosphorylated β-catenin by immediate EGF signaling (Fig. 6*B*, *right panel*) using anti-active β-catenin (ABC) antibody. Anti-ABC antibody recognizes non-phosphorylated Ser-37 and Thr-41 of β-catenin forms, which are resistant to proteasomal degradation (37). That the level of β-catenin was only slightly increased might have been due to the short EGF treatment time. The increment of p-EGFR by EGF was reduced by Axin induction. The levels of non-phosphorylated β-catenin, Ras, as well as the activities of the ERK pathway components, which were increased by EGF, were reduced by both induction of Axin and treatment of *EGFR* siRNA (Fig. 6*B*). Notably, we also observed reductions of both β-catenin and non-phosphorylated β-catenin by *EGFR* siRNA. We did not observe any changes in the levels of p-p38 under any of these conditions (Fig. 6*B*), which indicates specificity in the regulation of the β-catenin and ERK pathway components by EGFR, Axin etcetera.

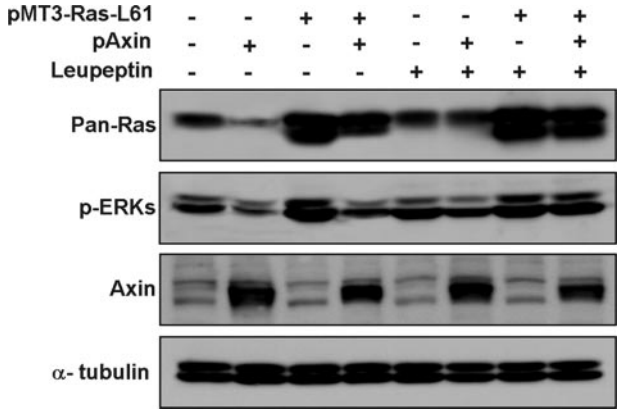

FIGURE 7. **Effect of leupeptin, a lysosomal inhibitor, on Ras degradation by Axin.** Chang cells were transfected with combination of vector, pAxin, and pMT3-H-Ras^{L61}. The cells were harvested at 24 h after transfection. In required cases, 10 μg/ml leupeptin was treated for 12 h before harvest cells. Pan-Ras, p-ERK, Axin, and α-tubulin were detected by Western blot analyses.

The Lysosomal Protein Degradation Machinery Is Involved in Ras Regulation by Axin—A recent study by Bar-Sagi's group (38) reported that mono- and di-ubiquitination of Ras is related to the endocytosis. To determine whether the endocytosis involves lysosomal degradation of Ras, we investigated the effect of leupeptin, a lysosomal inhibitor, in the regulation of the Ras protein level. Both endogenous Ras and overexpressed Ras^{L61}, which were reduced by Axin overexpression, were abolished in cells treated with leupeptin (Fig. 7). The lysosomal protein degradation machinery, then, is involved in Ras reduction by Axin.

Axin Inhibits Ras^{G12R}-induced but Not Raf-CAAX-induced Proliferation of L929 Fibroblast Cells—To determine whether Axin inhibits cellular proliferation and ERK pathway activation induced by Ras, we measured the effect of Axin transfection on BrdUrd incorporation stimulated by Dox-mediated induction of H-Ras^{G12R} in NIH3T3 fibroblast cells (39). The relative numbers of BrdUrd-positive cells were increased from 32% to 49% by H-Ras^{G12R} induction, but that increment was mostly abolished by transfection of the *Axin* gene (Fig. 8*A*). The proliferation of L929 cells was also increased by β-catenin gene transfection but was reduced by co-transfection of *Axin* (Fig. 8*B*), indicating as expected, that Axin inhibits proliferation induced by β-catenin. To further characterize a functional point of Axin in anti-proliferation by Axin, we measured the effects of Axin overexpression on the proliferation induced by Raf-CAAX, active Raf. The proliferation induced by overexpression of constitutively active Raf-1, Raf-1-CAAX, was not reduced by Axin induction (Fig. 8*C*), suggesting that Axin regulates the ERK pathway and proliferation upstream of Raf-1.

Axin Inhibits EGF-induced Anchorage-independent Growth of Fibroblasts—To determine whether Axin affects cellular transformation induced by ERK pathway activation, we measured the effect of GFP-Axin expression on colony formation induced by EGF. Under the no-EGF stimulation condition, the colony numbers formed by Axin-GFP-expressing cells were reduced by ~40% when compared with the numbers of control cells transfected with empty vector (Fig. 9). In addition, the size of colonies formed in GFP-Axin-expressing cells was reduced by ~45% (Fig. 9, representative data are shown in the *right*

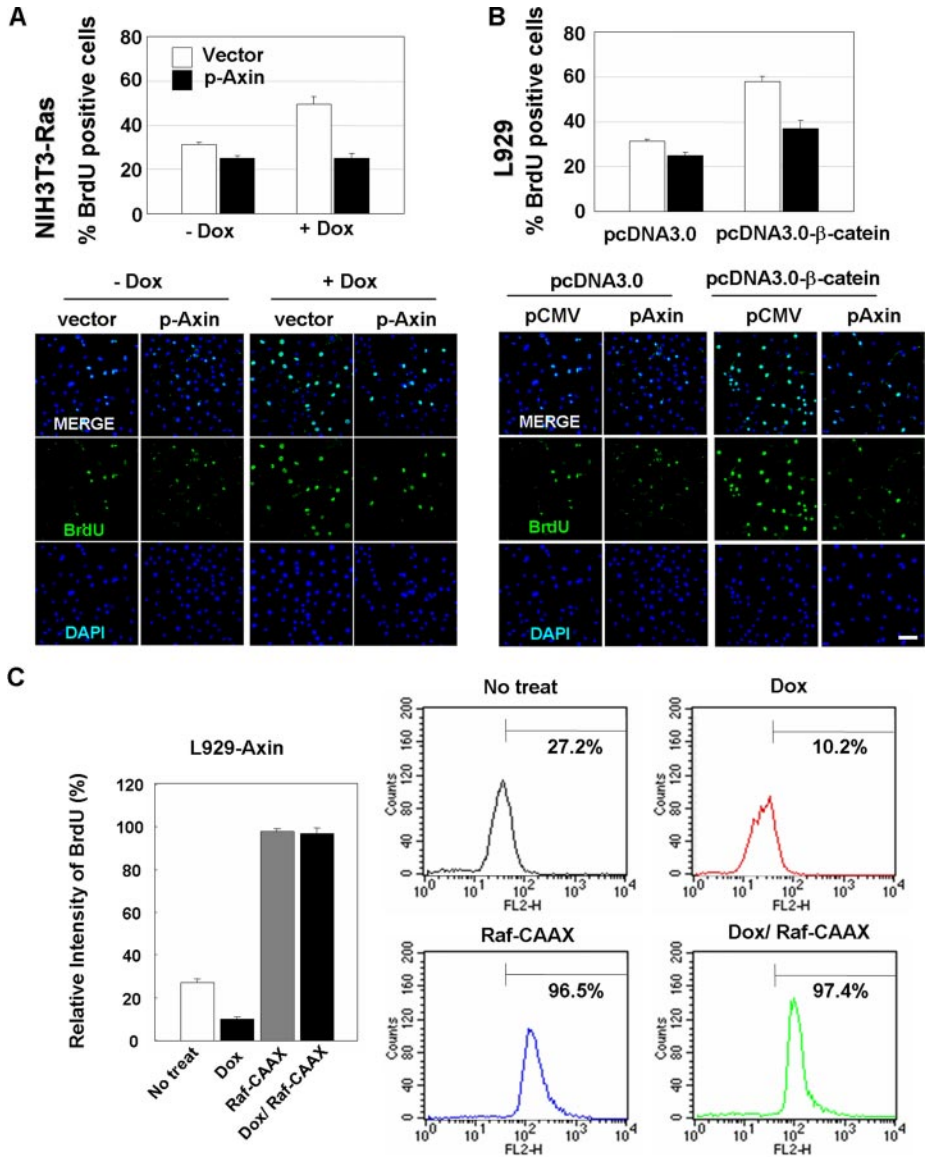

FIGURE 8. **Effects of Axin on Ras-, β-catenin-, or Raf-CAAX-induced proliferation.** *A*, NIH3T3 cells containing Dox-inducible H-*ras*^{G12R} were grown in DMEM containing 10% FBS at an 1×10^4 cells per well in 6-well plates. Cells were transiently transfected with either 0.5 μg/ml pCS2-MT or pCS2-MT-Axin. 12 h after transfection, cells were either untreated or treated with 0.5 μg/ml Dox for 24 h for Ras induction. 28 h after transfection, BrdUrd was added at a final concentration of 20 μM for 8 h. The cells were fixed, permeabilized, and incubated with anti-BrdUrd monoclonal antibody, followed by incubation with goat-anti-mouse-Cy^{TM2}-conjugated secondary antibody. Cell nuclei were stained with DAPI. Cells were visualized by a confocal microscope as described under "Experimental Procedures." Cells exhibiting BrdUrd incorporation in the nucleus were scored as BrdUrd-positive cells. *Error bars* indicate the standard deviations of three independent analyses. The *lower panel* shows representative results. *B*, L929 cells were co-transfected with either pcDNA3.0 or pcDNA3.0-FLAG-β-catenin and 0.5 μg of pCS2-MT or pCS2-MT-Axin. Cells were stained and analyzed as described in Fig. 8*A*. The percentage of BrdUrd-positive cells was calculated from the total number of DAPI-stained cells. Representative results are shown in the *lower panels*. *Bar*, 100 μM. *C*, L929-GFP-Axin cells were co-transfected with either vector or pZIP-Raf-CCAX. 12 h after transfection, the cells were either treated or untreated with 0.5 μg/ml Dox for 24 h for Axin induction. 28 h after transfection, BrdUrd was added at a final concentration of 20 μM for 8 h. The cells were fixed, permeabilized, and incubated with BrdUrd antibody, and subsequently with TRITC-conjugated goat anti-rabbit IgG. The relative intensities of TRITC-conjugated BrdUrd were measured using a FACS Vantage system (BD Biosciences Immunocytometry systems). Each data point represents the average of three independent analyses. Representative results are shown in the *right panels*.

panel). Compared with untreated cells, both the number and size of colonies formed by EGF treatment were increased ~2-fold, which were blocked by ectopic expression of GFP-Axin (Fig. 9). Moreover, the colony sizes were observed to be inversely correlated to the intensity of GFP-Axin (Fig. 9, *right panel*, compare *middle* and *lower boxes*).

DISCUSSION

Aberrant regulation of either the Wnt/β-catenin or the ERK pathway has been known to be implicated in many types of human cancers. However, the interaction between the two pathways in carcinogenesis is poorly understood. A defective *apc* allele and an activated *ras* gene are sufficient to transform normal colonic epithelial cells and render them carcinogenic (40). β-Catenin has been shown to cooperate with Ras in the development of colorectal cancer and hepatocellular carcinoma (22, 23). Simultaneous introduction of β-catenin gene and *ras* mutations into mice resulted in the development of hepatocellular carcinoma in 100% of tested animals, although neither *ras* nor β-catenin gene alone was sufficient for hepatocarcinogenesis (23). These results indicate that Wnt/β-catenin and ERK signaling experience cross-talk during carcinogenesis; however, the molecular details of how the two pathways can interact with each other remain poorly elucidated.

In this study, we investigated a mechanism for the Ras-ERK pathway regulation by Wnt/β-catenin signaling by modulating of the negative regulator Axin and related that mechanism to cellular proliferation and transformation. The ERK pathway components (Raf-1, MEK, and ERK kinases) were simultaneously lowered in cells in which the β-catenin level was reduced by Axin overexpression, indicating that Axin inhibits the Raf-1 → MEK → ERK cascade. Both EGF-induced G_1 to S phase progression and growth of L929 cells were also reduced by Axin overexpression, providing further evidence for the role of Axin in suppression of the cell growth that is controlled by the ERK pathway. The role of Axin in the inhibition of growth induced by the ERK pathway activation was further indicated by reduction of *ras*-induced proliferation by Axin. The sizes and numbers of colonies of L929 cells grown on a soft agar plate in the presence of

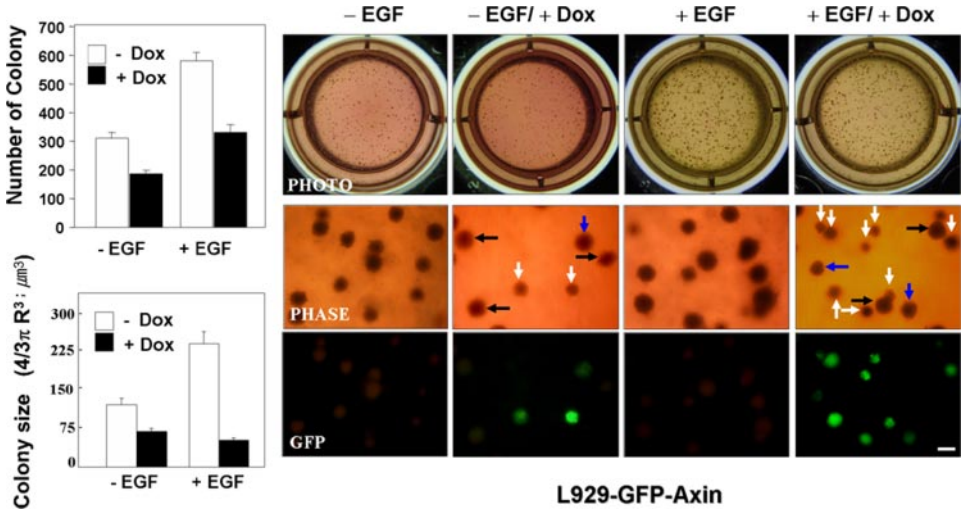

FIGURE 9. **Effects of Axin on EGF-induced transformation of L929 cells.** L929-GFP-Axin cells were grown in DMEM. The cells (1.2×10^3 cells/well in 12-well plates) were incubated for 14 days with or without 0.5 μg/ml Dox and/or 20 ng/ml EGF in soft agar. The average globe sizes and mean values of colony numbers (*left panel*) were calculated from at least 150 colonies as described under "Experimental Procedures." *Error bars* indicate the standard error-mean. Colonies expressing GFP-Axin were photographed under a phase-contrast fluorescence microscope. Cells not expressing GFP-Axin proteins are indicated by *black arrows*. Cells expressing an intermediate amount of GFP-Axin proteins are indicated by *blue arrows*. Cells expressing a high amount of GFP-Axin are marked by *white arrows*. *Bar*, 500 μm.

EGF were reduced by induction of Axin, indicating that Axin probably has an inhibitory function in transforming cellular growth induced by ERK pathway activation. The incidence of colony formation and the size of the formed colonies were both extremely low in the case of NIH3T3 cells compared with those of L-cells retaining transforming characteristics under identical growth conditions. Although the numbers were few, well developed small sized colonies were formed by induction of H-Ras^{G12R} by Dox (24). The H-Ras^{G12R}-induced colony formation was blocked by transfection of Axin (supplemental Fig. S2), confirming the role of Axin in anti-transformation of cells induced by oncogenic Ras.

The effects of Axin on the ERK pathway regulation was confirmed in similar analyses of primary hepatocytes, providing physiologically relevant evidence for down-regulation of the ERK signaling pathway by Axin. Inhibition of the ERK pathway components by *Axin* transfection occurred only in cells retaining wild-type β-catenin gene, including Chang liver cells and primary hepatocytes. The effects of *Axin* transfection on regulation of the ERK pathway components were not observed in cells, such as HCT-116 and HepG2 cancer cells, that harbored mutated β-catenin gene. The role of β-catenin in ERK pathway regulation by Axin was more convincingly confirmed by reduction of the activities of the ERK pathway components by siRNA-mediated reduction of non-degradable endogenous β-catenin in HCT-116 cells. Therefore, ERK pathway regulation by Axin probably occurs, at least partly, via regulation of β-catenin.

Currently, a mechanism for the ERK pathway regulation by Axin has yet to be clearly illustrated. The ERK activation by Ras^{L61} or β-catenin was lowered by dominant negative Tcf-4 (24, 41), indicating involvement of β-catenin/Tcf-mediated gene transcription in the ERK pathway regulation by Wnt/β-catenin signaling. The level of Ras-GTP was reduced by Axin overexpression, indicating that the Raf-1 → MEK → ERK regulation by Axin-β-catenin signaling occurs via Ras. Interestingly, the level of GTP-bound overexpressed non-hydrolyzable Ras^{L61} was also reduced by Axin overexpression, providing us an opportunity for identification of the regulation of the Ras protein level by Wnt/β-catenin signaling. Evidence for the Ras regulation by Axin was also provided by the reductions of the levels of endogenous Ras by Axin overexpression. A role of β-catenin in the regulation of the Ras protein level was also revealed by β-catenin-dependent degradation patterns in Ras regulation by Axin (Figs. 5*A*, 5*C*, and 6*A*). The Ras regulation by Axin was further confirmed by regulation of an activity of Akt, a known effecter of Ras (36), as well as the fact that the Akt regulation also occurred in cells retaining wild-type β-catenin gene (Fig. 6). The role of β-catenin in the regulation of Ras by Axin was also shown by regulation of the Ras level and activities of the ERK pathway components by knockdown of endogenous non-degradable mutant β-catenin (Fig. 5*C*). The loss of both Ras and ERK regulation by Axin in HCT-116 cells overexpressing non-degradable β-catenin S33Y further confirms the essential role of β-catenin in Ras regulation by Axin (Fig. 5*D*). Overall, the ERK pathway is subjected to dual Ras regulation, GTP loading, and Ras reduction by Axin. The theory explaining the dual regulation of Ras by Wnt/β-catenin signaling was supported by differences in the regulation folds between the Ras level and the activities of the ERK pathway components (Fig. 6*A*). The fold regulations of the ERK activities were much higher than those of the Ras protein level but similar to those of Ras-GTP. The level of Ras-GTP determines the fold regulation of the ERK pathway, because it represents the cumulative activity of Ras caused by regulation of GTP loading as well as by the level of Ras.

Currently, routes for regulations of the reduction and GTP loading of Ras are not clear. The regulation of GTP loading of Ras by Wnt/β-catenin signaling might be caused by the signal from upstream of Ras, and that explanation was supported by the recent identification of the epidermal growth factor receptor (EGFR) gene as a transcriptional target of Wnt/β-catenin signaling (42). However, we suggest that the major functional point of Axin in the regulation of the ERK pathway is Ras rather than EGFR. Axin inhibits Raf-1 → MEK → ERK cascade in cells retaining mutated *ras* as well as wild-type *ras*, indicating that Axin regulates Ras at least partly at its own level or downstream. The Ras^{L61}-induced proliferation was totally abolished (Fig. 8*A*), but the proliferation induced by constitutively active Raf-CAAX was not affected by Axin overexpression (Fig. 8*C*). These epistasis results further indicate that a functional point of Axin

in the regulation of the ERK pathway is Ras. We observed regulation of Ras by *EGFR* siRNA, however, that might be attributed by β-catenin regulation, as indicated by the concomitant reductions of β-catenin and Ras by *EGFR* siRNA (Fig. 6*B*). It is unknown how EGFR is involved in regulation of β-catenin, however, a previous study reported EGFR-β-catenin interaction without providing any information for cross-talk between Wnt/β-catenin and Ras-ERK pathways (43). The mechanism for Ras reduction by β-catenin signaling has also not been illustrated currently. However, a recent study has reported mono- and di-ubiquitination of Ras protein involving the endocytic pathway (38). The Ras reduction by Axin is potentially regulated by the lysosomal protein degradation machinery as indicated by inhibition of the Axin-induced Ras reduction by leupeptin in our current study.

In this study, we identified regulations of the Ras-ERK pathway and cellular proliferation and transformation by Wnt/β-catenin signaling involving Axin and its effector, β-catenin. The identification of Ras-ERK pathway regulation by Wnt/β-catenin signaling provides evidence for the role of the Ras-ERK pathway in tumorigenesis induced by abnormalities in Wnt/β-catenin signaling.

REFERENCES

1. Cadigan, K. M., and Nusse, R. (1997) *Genes Dev.* **11,** 3286–3305
2. Karim, R., Tse, G., Putti, T., Scolyer, R., and Lee, S. (2004) *Pathology* **36,** 120–128
3. Lustig, B., and Behrens, J. (2003) *J. Cancer Res. Clin. Oncol.* **129,** 199–221
4. Oving, I. M., and Clevers, H. C. (2002) *Eur. J. Clin. Invest.* **32,** 448–457
5. de La Coste, A., Romagnolo, B., Billuart, P., Renard, C. A., Buendia, M. A., Soubrane, O., Fabre, M., Chelly, J., Beldjord, C., Kahn, A., and Perret, C. (1998) *Proc. Natl. Acad. Sci. U. S. A.* **95,** 8847–8851
6. Miyoshi, Y., Iwao, K., Nagasawa, Y., Aihara, T., Sasaki, Y., Imaoka, S., Murata, M., Shimano, T., and Nakamura, Y. (1998) *Cancer Res.* **58,** 2524–2527
7. Laurent-Puig, P., Legoix, P., Bluteau, O., Belghiti, J., Franco, D., Binot, F., Monges, G., Thomas, G., Bioulac-Sage, P., and Zucman-Rossi, J. (2001) *Gastroenterology* **120,** 1763–1773
8. Taniguchi, K., Roberts, L. R., Aderca, I. N., Dong, X., Qian, C., Murphy, L. M., Nagorney, D. M., Burgart, L. J., Roche, P. C., Smith, D. I., Ross, J. A., and Liu, W. (2002) *Oncogene* **21,** 4863–4871
9. Lustig, B., Jerchow, B., Sachs, M., Weiler, S., Pietsch, T., Karsten, U., van de Wetering, M., Clevers, H., Schlag, P. M., Birchmeier, W., and Behrens, J. (2002) *Mol. Cell. Biol.* **22,** 1184–1193
10. Kinzler, K. W., and Vogelstein, B. (1996) *Cell* **87,** 159–170
11. Fearon, E. R., and Vogelstein, B. (1990) *Cell* **61,** 759–767
12. Behrens, J., Jerchow, B. A., Wurtele, M., Grimm, J., Asbrand, C., Wirtz, R., Kuhl, M., Wedlich, D., and Birchmeier, W. (1998) *Science* **280,** 596–599
13. Su, L. K., Vogelstein, B., and Kinzler, K. W. (1993) *Science* **262,** 1734–1737
14. Zeng, L., Fagotto, F., Zhang, T., Hsu, W., Vasicek, T. J., Perry, W. L., 3rd, Lee, J. J., Tilghman, S. M., Gumbiner, B. M., and Costantini, F. (1997) *Cell* **90,** 181–192
15. Kikuchi, A., Kishida, S., and Yamamoto, H. (2006) *Exp. Mol. Med.* **38,** 1–10
16. Giles, R. H., van Es, J. H., and Clevers, H. (2003) *Biochim. Biophys. Acta* **1653,** 1–24
17. Morin, P. J., Sparks, A. B., Korinek, V., Barker, N., Clevers, H., Vogelstein, B., and Kinzler, K. W. (1997) *Science* **275,** 1787–1790
18. Adjei, A. A. (2001) *J. Natl. Cancer Inst.* **93,** 1062–1074
19. Fang, J. Y., and Richardson, B. C. (2005) *Lancet Oncol.* **6,** 322–327
20. Vogelstein, B., Fearon, E. R., Hamilton, S. R., Kern, S. E., Preisinger, A. C., Leppert, M., Nakamura, Y., White, R., Smits, A. M., and Bos, J. L. (1988) *N. Engl. J. Med.* **319,** 525–532
21. Jen, J., Powell, S. M., Papadopoulos, N., Smith, K. J., Hamilton, S. R., Vogelstein, B., and Kinzler, K. W. (1994) *Cancer Res.* **54,** 5523–5526
22. Damalas, A., Kahan, S., Shtutman, M., Ben-Ze'ev, A., and Oren, M. (2001) *EMBO J.* **20,** 4912–4922
23. Harada, N., Oshima, H., Katoh, M., Tamai, Y., Oshima, M., and Taketo, M. M. (2004) *Cancer Res.* **64,** 48–54
24. Park, K. S., Jeon, S. H., Kim, S. E., Bahk, Y. Y., Holmen, S. L., Williams, B. O., Chung, K. C., Surh, Y. J., and Choi, K. Y. (2006) *J. Cell Sci.* **119,** 819–827
25. Lyu, J., Costantini, F., Jho, E. H., and Joo, C. K. (2003) *J. Biol. Chem.* **278,** 13487–13495
26. Marais, R., Light, Y., Paterson, H. F., and Marshall, C. J. (1995) *EMBO J.* **14,** 3136–3145
27. Brummelkamp, T. R., Bernards, R., and Agami, R. (2002) *Cancer Cell* **2,** 243–247
28. Kolligs, F. T., Hu, G., Dang, C. V., and Fearon, E. R. (1999) *Mol. Cell. Biol.* **19,** 5696–5706
29. Woodcroft, K. J., and Novak, R. F. (1999) *Biochem. Biophys. Res. Commun.* **266,** 304–307
30. Salahshor, S., and Woodgett, J. R. (2005) *J. Clin. Pathol.* **58,** 225–236
31. Tetsu, O., and McCormick, F. (1999) *Nature* **398,** 422–426
32. Ikeda, S., Kishida, S., Yamamoto, H., Murai, H., Koyama, S., and Kikuchi, A. (1998) *EMBO J.* **17,** 1371–1384
33. Ilyas, M., Tomlinson, I. P., Rowan, A., Pignatelli, M., and Bodmer, W. F. (1997) *Proc. Natl. Acad. Sci. U. S. A.* **94,** 10330–10334
34. Carruba, G., Cervello, M., Miceli, M. D., Farruggio, R., Notarbartolo, M., Virruso, L., Giannitrapani, L., Gambino, R., Montalto, G., and Castagnetta, L. (1999) *Ann. N. Y. Acad. Sci.* **886,** 212–216
35. Bos, J. L. (1989) *Cancer Res.* **49,** 4682–4689
36. Campbell, P. M., and Der, C. J. (2004) *Semin. Cancer Biol.* **14,** 105–114
37. van Noort, M., Meeldijk, J., van der Zee, R., Destree, O., and Clevers, H. (2002) *J. Biol. Chem.* **277,** 17901–17905
38. Jura, N., Scotto-Lavino, E., Sobczyk, A., and Bar-Sagi, D. (2006) *Mol. Cell* **21,** 679–687
39. Lim, Y., Han, I., Jeon, J., Park, H., Bahk, Y. Y., and Oh, E. S. (2004) *J. Biol. Chem.* **279,** 29060–29065
40. D'Abaco, G. M., Whitehead, R. H., and Burgess, A. W. (1996) *Mol. Cell. Biol.* **16,** 884–891
41. Yun, M. S., Kim, S. E., Jeon, S. H., Lee, J. S., and Choi, K. Y. (2005) *J. Cell Sci.* **118,** 313–322
42. Tan, X., Apte, U., Micsenyi, A., Kotsagrelos, E., Luo, J. H., Ranganathan, S., Monga, D. K., Bell, A., Michalopoulos, G. K., and Monga, S. P. (2005) *Gastroenterology* **129,** 285–302
43. Takahashi, K., Suzuki, K., and Tsukatani, Y. (1997) *Oncogene* **15,** 71–78